

Syntheses and molecular structures of group 8 benzonitrile complexes

Richard L. Cordiner, David Albesa-Jové, Rachel L. Roberts, Julian D. Farmer,
Horst Puschmann, Deborah Corcoran, Andrés E. Goeta, Judith A.K. Howard, Paul J. Low *

Department of Chemistry, University of Durham, South Rd, Durham DH1 3LE, UK

Received 12 April 2005; received in revised form 26 July 2005; accepted 3 August 2005
Available online 19 September 2005

Abstract

The molecular structures of eight nitrile complexes of general form $[M(NCC_6H_4R-4)(L_2)Cp']PF_6$ [$M = Fe, Ru$; $L_2 = dppe, (PPh_3)_2$; $Cp' = Cp, Cp^*$] are reported and discussed in terms of the nature of the M–N interaction. Data are consistent with a predominantly σ -interaction, similar to that found in related acetylide complexes, with little evidence for metal to nitrile π -back bonding interactions. © 2005 Elsevier B.V. All rights reserved.

Keywords: Nitrile; Back-bonding; Molecular structure

1. Introduction

The interest in nitrile ligand chemistry has undergone something of a renaissance in recent years, spurred on by observations of significant second order non-linear optical responses [1–8], the desire to rationalise and exploit the greatly enhanced electrophilicity of the nitrile carbon centre when coordinated to an electron-rich metal centre [9–11], and the rigid-rod like structure of the M–N–C moiety [12]. Nitriles are isoelectronic with acetylide anions and, unsurprisingly, similar interests have prompted many investigations of the synthesis, molecular structure, reactivity, optical and magnetic properties and electronic structure of metal acetylide complexes [13–17].

We have recently undertaken an investigation of the coordination and organometallic chemistry of a number of unusual cyanocarbons [18], and have described the synthesis of complexes $[Ru(N\equiv CC\equiv CPh)(PPh_3)_2Cp][PF_6]$ and $Ru(C\equiv CC\equiv N)(PPh_3)_2Cp$, featuring the cyanoacetylene and cyanoacetylide ligands, respectively [19]. While the phenylpropionitrile ligand is readily displaced by other donor ligands including NCMe and tetracyanoethene

(TCNE), the cyanoacetylide complex is a much stronger σ -donor, and can be used in the formation of robust homo and hetero-bimetallic compounds such as $[\{Ru(PPh_3)_2Cp\}_2(\mu-C\equiv CC\equiv N)][PF_6]$ and $[\{Cp(PPh_3)_2Ru\}(\mu-C\equiv CC\equiv N)\{Fe(dppe)Cp\}][PF_6]$. In the course of extending this study to other half-sandwich metal systems, and exploring the nature of the M–N \equiv CC \equiv CR bonding interaction, we found it necessary to have access to a range of spectroscopic, electrochemical and structural parameters from simple nitrile complexes of general form $[M(NCR)-(L_2)(\eta^5-C_5R'_2)]^+$. We report here a number of these half-sandwich complexes featuring benzonitrile ligands, and offer a comparison of the structural and electronic trends within the series.

2. Results and discussion

A wide variety of nitriles have been shown to displace the halide ligand (X) from iron and ruthenium complexes $MX(L_2)Cp$ to afford cations $[M(NCR)(L_2)Cp]^+$, which are readily isolated as the corresponding BF_4^- or PF_6^- salts from reactions carried out in methanol or acetone [1–4,6,7,17,20–22]. The complex salts $[Ru(NCPh)(PPh_3)_2Cp][PF_6]$ (**1**), $[Ru(NCPh)(dppe)Cp^*][PF_6]$ (**2**) and $[Fe(NCPh)(dppe)Cp][PF_6]$ (**3**) (Chart 1) were synthesised in good yield from the reaction of the corresponding chloride complexes with

* Corresponding author. Tel.: +44 0191 334 2114; fax: +44 0191 374 4737.

E-mail address: p.j.low@durham.ac.uk (P.J. Low).

a 3-fold excess of benzonitrile in methanol solutions containing NH_4PF_6 , and crystallised by slow diffusion of methanol (**1**, **3**) or hexane (**2**) into concentrated CH_2Cl_2 solutions. The substituted derivatives $[\text{Ru}(\text{NCC}_6\text{H}_4\text{NO}_2\text{-4})\text{(PPh}_3)_2\text{Cp}]\text{PF}_6$ (**4**) and $[\text{Ru}(\text{NCC}_6\text{H}_4\text{NMe}_2\text{-4})\text{(PPh}_3)_2\text{Cp}]\text{PF}_6$ (**5**) were readily prepared in an entirely analogous procedure from the stoichiometric reaction of $\text{RuCl}(\text{PPh}_3)_2\text{Cp}$ with 4-nitrobenzonitrile or 4-(dimethylamino)benzonitrile, respectively. In the case of the reaction with 1,4-dicyanobenzene (terephthalonitrile), the stoichiometric reaction to form $[\text{Ru}(\text{NCC}_6\text{H}_4\text{CN})\text{(PPh}_3)_2\text{Cp}]\text{PF}_6$ (**6a**) was complicated by the tendency for further reaction and/or disproportionation to afford the bimetallic dicationic complex $[\{\text{Ru}(\text{PPh}_3)_2\text{Cp}\}_2(\mu\text{-NCC}_6\text{H}_4\text{CN})]\text{PF}_6$ (**7**). In order to prepare pure samples of **6a** it proved necessary to employ a large (10-fold) excess of terephthalonitrile to metal reagent, while complex **7** could be readily obtained either by reaction of **6a** with a further equivalent of $\text{RuCl}(\text{PPh}_3)_2\text{Cp}$, or directly from the reaction of terephthalonitrile with one half equivalent of the ruthenium precursor. The iron analogue of **7**, $[\{\text{Fe}(\text{dppe})\text{Cp}\}_2(\mu\text{-NCC}_6\text{H}_4\text{CN})]\text{PF}_6$ (**8**) was prepared directly from the stoichiometric reaction of $\text{FeCl}(\text{dppe})\text{Cp}$ with terephthalonitrile in THF containing NH_4PF_6 , and isolated as a bright red crystalline material following crystallisation ($\text{CH}_2\text{Cl}_2/\text{Et}_2\text{O}$). The sample analysed consistently with one molecule of CH_2Cl_2 per formula unit, with the solvent of crystallisation also being observed in the ^1H NMR spectrum of the product.

Reaction of 4-ethynylbenzonitrile with $\text{RuCl}(\text{PPh}_3)_2\text{Cp}$ and NH_4PF_6 followed by treatment with NaOMe to deprotonate the intermediate vinylidene, gave the acetylide complex $[\text{Ru}(\text{C}\equiv\text{CC}_6\text{H}_4\text{CN})\text{(PPh}_3)_2\text{Cp}]$ (**6b**), which is isoelectronic with **6a**. Complex **6b** reacted smoothly with a further equivalent of $\text{RuCl}(\text{PPh}_3)_2\text{Cp}$ to give the bimetallic complex $[\{\text{Cp}(\text{PPh}_3)_2\text{Ru}\}_2(\mu\text{-C}\equiv\text{CC}_6\text{H}_4\text{CN})]\text{PF}_6$ (**9**). Complex **9** could also be prepared directly from 4-ethynylbenzonitrile and two equivalents of $\text{RuCl}(\text{PPh}_3)_2\text{Cp}$ in the presence of NH_4PF_6 and subsequent treatment with base.

The availability of the cluster substituted benzonitrile $[\text{Co}_2(\mu\text{-HC}_2\text{C}_6\text{H}_4\text{CN-4})(\text{CO})_4(\text{dppm})]$ prompted us to examine the coordination reaction of this species to the $\text{Ru}(\text{PPh}_3)_2\text{Cp}$ as well. The reaction with $\text{RuCl}(\text{PPh}_3)_2\text{Cp}$ proceeded in a manner entirely analogous to that described above, although the low solubility of the cobalt cluster $\text{Co}_2(\mu\text{-HC}_2\text{C}_6\text{H}_4\text{CN-4})(\text{CO})_4(\text{dppm})$ in methanol necessitated the use of a THF/methanol co-solvent in the preparation of $[\text{Co}_2(\mu\text{-HC}_2\text{C}_6\text{H}_4\text{CN}\{\text{Ru}(\text{PPh}_3)_2\text{Cp})\}(\text{CO})_4(\text{dppm})]\text{PF}_6$ (**10**).

The complex salts were readily characterised by the usual spectroscopic methods, and pertinent data are summarised in Table 1. Some earlier studies suggested a significant contribution from π -back bonding effects in the nitrile complexes of strongly electron donating metal fragments such as ML_2Cp ($\text{M} = \text{Fe}, \text{Ru}$; $\text{L} = \text{phosphine}$) to explain the spectroscopic properties of metal nitrile complexes, which include shifts of the IR active $\nu(\text{C}\equiv\text{N})$ bands

to lower energy relative to the respective free ligands in many cases [2,4,6–8,22]. However, more recently computational studies have indicated only a minimal contribution from π -back bonding to the overall electronic structure, suggesting instead that the various spectroscopic and structural properties of these complexes may be attributed to orbital polarisation and electrostatic effects transmitted through the M-N σ -bond [9–11].

In the ruthenium based complexes studied here, the $\nu(\text{C}\equiv\text{N})$ stretch in the coordinated nitrile ligand (recorded with 2 cm^{-1} resolution) was found to fall in the narrow range 2221 (**5**, **6a**)–2233 (**1**) cm^{-1} and within ca. $\pm 10\text{ cm}^{-1}$ of the $\nu(\text{C}\equiv\text{N})$ band in the free ligand. The observed shifts do not correlate with trends which might be expected on the basis of the π -character of the nitrile ligand substituent. For example, the $\nu(\text{C}\equiv\text{N})$ band of **5**, which features the electron donating NMe_2 group, was found at the same frequency as the $\nu(\text{C}\equiv\text{N})$ band in the CN substituted derivative **6a**, and at a slightly lower frequency than the NO_2 substituted derivative **4**.

A more systematic variation was found in the position of $\nu(\text{CN})$ band as a function of the metal fragment within the series **1** (2233 cm^{-1}), **2** (2227 cm^{-1}), **3** (2217 cm^{-1}). The decreased $\nu(\text{C}\equiv\text{N})$ frequency in iron nitrile complexes relative to ruthenium examples has previously been attributed to the greater π -donating ability of the iron centre and enhanced back-bonding from the metal to ligand [4,6,7]. However, given the identical N-C bond lengths in the series (see below) it may not be wise to simply analyse this subtle decrease in $\nu(\text{C}\equiv\text{N})$ stretching frequency in terms of variations in π -back bonding effects alone [9–11].

The ^{31}P NMR chemical shifts of the triphenylphosphine ligands and the ^1H and ^{13}C resonances of the Cp ligand displayed a discernable variation in chemical shift with the inductive nature of the *para* substituent. Such trends are common in half-sandwich complexes of this type, and the variations in chemical shift with electron density at the metal centre correlate with those observed in the isoelectronic acetylide complexes such as $\text{Fe}(\text{C}\equiv\text{CC}_6\text{H}_4\text{X-4})(\text{dppe})\text{Cp}^*$ [23] and $\text{Ru}(\text{C}\equiv\text{CC}_6\text{H}_4\text{X-4})(\text{PPh}_3)_2\text{Cp}$ [24] with more electron donating substituents leading to lower frequency resonances.

The electrochemical response of the complexes should also reflect the relative donor ability of the ligands and the metal centre. Cyclic voltammetry (CV) studies were performed on each of the compounds **1–9** using a platinum disc working electrode and platinum wire counter and pseudo-reference electrodes, from CH_2Cl_2 solutions containing 0.1 M $[\text{N}(\text{C}_4\text{H}_9)_4][\text{BF}_4]$, with electrode potentials cited against an internal ferrocene ($\text{Fc}/\text{Fc}^+ = 0.46\text{ V}$ vs. SCE) or decamethylferrocene ($\text{Fc}^*/\text{Fc}^{*+} = -0.02\text{ V}$ vs. SCE) standard [25]. The electrochemical response of **1** at a platinum electrode was characterised by a single oxidation event at +1.30 V, the chemical reversibility of which was improved at sub-ambient temperatures. Compounds **2** and **3** both displayed reversible oxidation waves at +1.10 and +0.83 V, respectively, with the lower oxidation

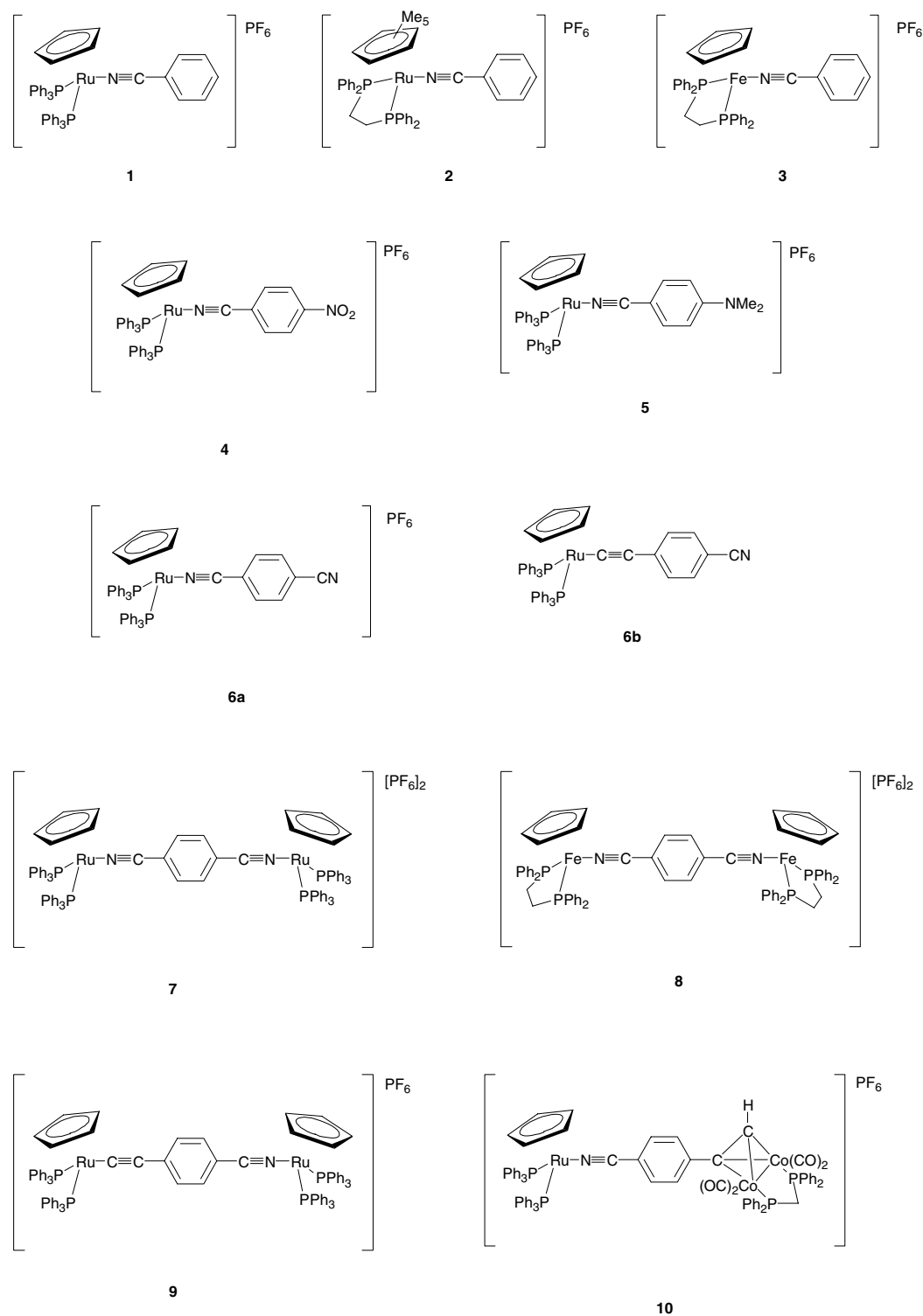


Chart 1. The complexes employed in this study.

potentials relative to **1** reflecting the more electron donating supporting ligands surrounding the metal centres. Compounds **4**, **5**, **6a** and **7** each displayed an irreversible, poorly defined oxidation event, the shape of which could not be improved even at sub-ambient temperatures and scan rates up to 5 V/s.

The bis(iron) complex **8** gave rise to two sequential oxidation processes ($E_{1/2} = 0.84, 0.91$ V), the separation of which (ΔE ca. 70 mV) indicates the metal centres to be essentially independent [26]. The small separation of the electrochemical events contrasts dramatically with the relatively large ($\Delta E = 260$ mV, $K_c = 2.6 \times 10^4$) separation of

Table 1

Selected spectroscopic data for complexes and ligands reported in this work (NMR spectra in CDCl₃ unless otherwise indicated)

Compound	$\nu(\text{C}\equiv\text{N}) \text{ cm}^{-1}$	Cp $\delta_{\text{H}}/\delta_{\text{C}}$	C≡N δ_{C}	C1	C2	C3	C4	PR ₃ δ_{P}	Reference
N≡CC ₆ H ₅	2229		118.39	111.97	131.66	128.75	132.41		[6]
N≡CC ₆ H ₄ NO ₂	2240		116.69	118.13	133.38	124.13	149.88		[6]
N≡CC ₆ H ₄ NMe ₂	2210		120.48	96.84	133.01	111.16	152.23		[6]
N≡CC ₆ H ₄ C≡N			116.96 ^a	116.72 ^a	132.76				
1	2233	4.55/84.38	Not obs.	111.50	132.73	129.49	133.82	42.89	
2 ^c	2227	^b		111.26				76.15	
3	2217	4.45	129.13	111.41	133.35	132.04	134.32	98.32	
4	2228	4.64/84.98	127.91	117.46	124.31	134.21	150.04	42.97	
5	2221	4.42/83.81	Not obs.	95.61	133.84	111.77	153.23	42.82	
6a	2221	4.62						42.58	
6b	2220 ^c	4.31/85.76	120.70	115.91	131.07	131.92	135.29	51.25	
7 ^f	2226	4.57						42.58	
8	2223	4.47/80.45	Not obs.	114.69	131.39 ^a	130.97 ^a		97.90	
9	2218 ^d	4.34, 4.51/83.93, 85.79	Not obs.	116.96	131.77	131.05	Not obs.	42.84, 51.25	

^a Or vice versa.^b Cp* δ_{H} 1.51 ppm, δ_{C} 93.18, 9.68 ppm.^c $\nu(\text{C}\equiv\text{C})$ 2063, 2037sh cm^{-1} .^d 2059, 2040sh cm^{-1} .^e In CD₂Cl₂.^f Limited solubility precluded the observation of ¹³C NMR resonances in common solvents.

the oxidation processes observed in the related 1,4-diethynyl benzene bridged species [$\{\text{Fe}(\text{dppe})\text{Cp}^*\}_2(\mu\text{-C}\equiv\text{CC}_6\text{-H}_4\text{C}\equiv\text{C})$] [27], and consequently the high thermodynamic stability of the mono-oxidised form of the bis(acetylide) complex towards disproportionation [26].

Compound **9** displayed a reversible oxidation wave at +0.73 V and a second irreversible wave ($E_{\text{p}} = +1.45$ V) that resulted in the formation of a deposit on the electrode precluding further characterisation of this wave. As the analogous mononuclear acetylide complex **6b** was characterised by a single oxidation event at +0.71 V, the chemical reversibility of which was improved at sub-ambient temperatures, the reversible process observed in **9** is assigned to an oxidation event predominantly localised on the metal acetylide fragment.

The electronic absorption spectra of each compound with the exception of **6a** (due to the disproportionation problems described above) and **2** (which proved to be

insoluble in THF) were recorded as 0.1 mM solutions in both CH₂Cl₂ and THF (Table 2). Each compound exhibited an absorption band with a λ_{max} in the range 240–260 nm which displayed no solvatochromic behaviour and was assigned to the localised π/π^* transitions of the phosphine ligands. Similar assignments have been made previously for a series of closely related compounds [28,29]. In addition, each compound gave rise to a broad envelope between 300 and 450 nm. This envelope contained two absorption bands, the relative positions and intensities of which varied between complexes. In the case of compounds **1**, **4**, **5** and **7** these bands overlapped to such an extent that it was impossible to establish the positions of the two separate band maxima and the only distinguishable maximum is reported here. In the remaining cases, however, it was possible to distinguish two band maxima in the 300–450 nm region. These were tentatively assigned as MLCT Ru_d π -Cp for the higher energy

Table 2

UV/Vis absorption data from complexes **1–5** and **7–10**

Complex	$\lambda_{\text{max}}/\text{nm}$ ($\epsilon/\text{M}^{-1} \text{ cm}^{-1}$) (CH ₂ Cl ₂)	$\lambda_{\text{max}}/\text{nm}$ ($\epsilon/\text{M}^{-1} \text{ cm}^{-1}$) (THF)
1	238 (52,900), 307 (13,600)	230 (70,400), 307 (13,500)
2	249 (26,900), 310 (8400), 346 (6600)	n/a
3	258 (17,800), 328 (5600), 391 (2500)	260 (17,100), 331 (5900), 391 (3200)
4	237 (43,200), 384 (6900)	229 (51,000), 329 (6900)
5	230 (62,700), 332 (55,000)	234 (45,400), 332 (45,000)
7	247 (85,400), 363 (20,900), 420 (17,100)	225 (55,600), 363 (10,300), 420 (8300)
8	227 (1,38,500), 450 (4600)	210 (259,000), 463 (9000)
9	240 (81,500), 415 (24,510)	240 (29,100), 410 (26,000)
10	270 (30,800), 360 (15,200), 550 (2400)	270 (55,400), 360 (29,500), 550 (1800)

transition, which seems to be too intense to be assigned to d–d processes, and MLCT $\text{Ru}_{\text{d}\pi}\text{--NCR}_{\pi^*}$ for the lower. Comparable transitions in the iron complexes **3** and **8** are assigned similarly. The marked solvatochromic nature of the lowest energy band in compound **4** (which bears the strongly electron-withdrawing NO_2 group) supports this assignment.

Single crystals of the nitrile complexes **2**, **3**, **4**, **5**, **7**, **9** and **10** and the acetylide complex **6b** were obtained by slow diffusion of methanol or hexane into concentrated CH_2Cl_2 solutions of the complex salt. Crystallographic details are summarised in Table 3, while important bond lengths and angles are summarised in Table 4, together with those of some closely related species reported earlier by others. Plots of individual ions and molecules are illustrated in Figs. 1–8 and show the atomic labelling schemes employed. The structural analyses reveal the expected half-sandwich metal fragments, with the average M–C (Cp or Cp*) distances being somewhat shorter in the case of the nitrile complexes than the acetylides.

The structure of the benzonitrile complex **1** has been reported on a previous occasion [19], and the metrical parameters of this compound provide a useful point for comparison. Substitution of the Cp and PPh_3 ligands in **1** for Cp* and dppe ligands in **2** (Fig. 1) results in an increase in the electron density at the metal centre (as evidenced by the lower oxidation potential of **2** vs. **1**). Interestingly, this increase in electron density results in contraction of the Ru–P bonds through enhanced $\text{Ru} \rightarrow \text{P}$ back bonding, rather than any significant foreshortening of the Ru–N contact. The coordinated nitrile $\text{N}\equiv\text{C}$ bond lengths are identical in **1** and **2**, and the only other significant change in bond lengths and angles is the smaller P–Ru–P angle in **2** which is a consequence of the ethyl bridge in the diphosphine ligand.

The shorter Fe–N bond length in **3** (Fig. 2) compared with the ruthenium species **1** and **2** reflects the smaller size of the iron atom, and the bond parameters associated with **3** are better compared with those of the complex cation $[\text{Fe}(\text{NCC}_6\text{H}_4\text{NO}_2)(\text{dppe})\text{Cp}]^+$ (Fe–N 1.874(11) Å [30]), and the Fe–N contacts in these two complexes are found to be indistinguishable within the limits of precision of the structure solutions.

The C–N(O_2) bond length in **4** [1.490(8)–1.523(11) Å], the NO_2 group being disordered over three sites] (Fig. 3) is similar to that found in the free ligand [1.48(1) Å] [31] and significantly longer than in the related acetylide complex $\text{Ru}(\text{C}\equiv\text{CC}_6\text{H}_4\text{NO}_2)(\text{PPh}_3)_2\text{Cp}$ [1.468(6) Å] [24], and the iron complex $\text{Fe}(\text{C}\equiv\text{CC}_6\text{H}_4\text{NO}_2)(\text{dppe})\text{Cp}$ [1.455 Å] [23]. The Ru–N bond length in **4** is somewhat shorter than in the parent benzonitrile species **1**, although the difference between **4** and **5**, which features the NMe_2 group, is at the borderline of statistical significance and must therefore be regarded with caution.

There are surprisingly few other examples of metal complexes of *N,N*-dimethylaminobenzonitrile to facilitate more detailed comparisons [32]. The C–NMe₂ distance

Table 3
Summary of crystal data for complexes **1–5**, **6b**, **7**, **9**, **10**

Compound	2	3	4	5	6b	7	9	10
Formula	$\text{C}_{43}\text{H}_{44}\text{F}_6\text{NP}_3\text{Ru}$	$\text{C}_{38}\text{H}_{34}\text{F}_6\text{NP}_3\text{Fe}$	$\text{C}_{48}\text{H}_{39}\text{F}_6\text{N}_2\text{P}_3\text{O}_2\text{Ru} \cdot \text{CH}_2\text{Cl}_2$	$\text{C}_{50}\text{H}_{45}\text{F}_6\text{N}_2\text{P}_3\text{Ru}$	$\text{C}_{50}\text{H}_{39}\text{NP}_2\text{Ru}$	$\text{C}_{90}\text{H}_{74}\text{F}_{12}\text{N}_2\text{P}_6\text{Ru}_2 \cdot 2\text{CH}_2\text{Cl}_2$	$\text{C}_{91}\text{H}_{74}\text{F}_6\text{NO}_2\text{P}_3\text{Ru}_2 \cdot 2\text{C}_3\text{H}_6\text{O}$	$\text{C}_{79}\text{H}_{62}\text{Co}_2\text{F}_6\text{NO}_4\text{P}_3\text{Ru} \cdot 0.6\text{CH}_2\text{Cl}_2$
Formula weight	882.77	767.42	1068.72	981.86	816.83	1969.32	1765.66	
<i>a</i> (Å)	11.8209(6)	10.5129(5)	13.4710(11)	11.4435(5)	12.9540(3)	17.9679(7)	13.5570(18)	13.6667(18)
<i>b</i> (Å)	17.8172(9)	16.4328(8)	18.9603(13)	13.8495(7)	16.7588(4)	16.5775(7)	18.406(3)	16.392(2)
<i>c</i> (Å)	19.7578(10)	20.0776(10)	18.1940(14)	15.2404(7)	17.5894(4)	28.5453(12)	18.554(2)	16.958(2)
α (°)	90	90	90	87.187(2)	90	90	63.479(2)	98.113(4)
β (°)	92.623(2)	90	95.816(4)	72.213(2)	90	90	79.126(2)	105.243(4)
γ (°)	90	90	90	73.038(2)	90	90	82.183(3)	97.515(4)
<i>V</i> (Å ³)	4156.9(4)	3468.5(3)	4623.1(6)	2197.76(18)	3818.54(15)	8502.6(6)	4061.2(9)	3572.1(8)
ρ (mg/m ³)	1.411	1.470	1.535	1.484	1.421	1.538	1.446	1.519
<i>T</i> (K)	120(2)	120(2)	120(2)	120(2)	120(2)	120(2)	120(2)	120(2)
Crystal system	Monoclinic	Orthorhombic	Monoclinic	Triclinic	Orthorhombic	Orthorhombic	Triclinic	Triclinic
Space group	$P2_1/n$	$P2_12_12_1$	$P2_1/n$	$P\bar{1}$	$P2_12_12_1$	<i>pbca</i>	$P\bar{1}$	$P\bar{1}$
<i>Z</i>	4	4	4	2	4	4	2	2
μ (mm ^{−1})	0.550	0.635	0.625	0.530	0.532	0.669	0.536	0.893
Reflections collected	38,442	32,697	37,877	31,076	42,399	81,098	42,161	42,947
Independent reflections [R_{int}]	12,677 [0.0452]	10,550 [0.0375]	11,417 [0.0299]	13,334 [0.0203]	8778 [0.0379]	9288 [0.0683]	21,594 [0.0846]	17,982 [0.0324]
Final <i>R</i> indices (all data)	$R_1 = 0.1184$ $wR_2 = 0.3299$	$R_1 = 0.0512$ $wR_2 = 0.1037$	$R_1 = 0.0396$ $wR_2 = 0.0741$	$R_1 = 0.0395$ $wR_2 = 0.0863$	$R_1 = 0.0247$ $wR_2 = 0.0556$	$R_1 = 0.0551$ $wR_2 = 0.0971$	$R_1 = 0.1687$ $wR_2 = 0.1436$	$R_1 = 0.0589$ $wR_2 = 0.1147$

Table 4
Selected bond lengths and angles for compounds **1–5**, **6b**, **7**, **9**, **10** and related species

Compound	M–E	E≡C	C–C(ipso)	M–P(1)	M–P(2)	M–E–C	E–C–C(ipso)	P(1)–M–P(2)	
PhCN		1.137(14)	1.401(14)				180.00		[36]
NCC ₆ H ₄ NO ₂ -4		1.155(15)	1.438(15)				179(1)		[31]
NCC ₆ H ₄ NMe ₂ -4		1.145(3)	1.434(4)				179.49		[33]
[Ru(NCPh)(PPh ₃) ₂ Cp]PF ₆ 1	2.037(1)	1.145(2)	1.440(2)	2.334(1)	2.335(1)	171.70(12)	177.84(16)	97.46(1)	This work
[Ru(NCPh)(dppe)Cp*]PF ₆ 2	2.027(5)	1.146(7)	1.438(7)	2.315(1)	2.315(1)	173.6(4)	174.9(6)	83.50(5)	This work
[Ru(NCC ₆ H ₄ NO ₂)(PPh ₃) ₂ Cp]PF ₆ 4	2.023(2)	1.146(2)	1.442(3)	2.329(1)	2.330(1)	171.24(15)	177.8(2)	100.30(2)	This work
[Ru(NCC ₆ H ₄ NO ₂){(+)-DIOP}Cp]PF ₆	2.031(13)	1.137(18)	1.42(2)	2.330(4)	2.309(4)	177.2(12)	178.6(15)	96.48(12)	[8]
[Ru(NCC ₆ H ₄ NMe ₂)(PPh ₃) ₂ Cp]PF ₆ 5	2.031(1)	1.149(2)	1.424(2)	2.325(1)	2.321(1)	173.52(14)	175.15(18)	104.24(2)	This work
[Ru(NCC ₆ H ₄ OEt)(PPh ₃) ₂ Cp]PF ₆	2.041(5)	1.152	1.405	2.352	2.337	175.6	175.1	100.6	[3]
Ru(C≡CPh)(PPh ₃) ₂ Cp	2.016(3)/ 2.017(5)	1.215(4)/ 1.214(7)	1.456(4)/ 1.462(8)	2.303/ 2.229(3)	2.285/ 2.228(3)	178.0(2)/ 177.7(4)	171.9(3)/ 170.6(5)	100.5/ 100.9(1)	[37]/[38]
Ru(C≡CC ₆ H ₄ NO ₂)(PPh ₃) ₂ Cp 4	1.994(5)	1.202(8)	1.432(7)	2.297(2)	2.301(2)	175.9(4)	175.0(9)	101.17(7)	[24]
Ru(C≡CC ₆ H ₄ CN)(PPh ₃) ₂ Cp 6b	2.011(2)	1.219(3)	1.432(3)	2.3134(5)	2.3031(5)	175.43(18)	175.1(2)	102.21(2)	This work
[Fe(NCPh)(dppe)Cp]PF ₆ 3	1.892(2)	1.141(3)	1.444(3)	2.207(1)	2.206(1)	172.16(18)	174.5(2)	84.37(6)	This work
[Fe(NCC ₆ H ₄ NO ₂)(dppe)Cp]PF ₆	1.874(11)	1.129(14)	1.42(2)	2.210(4)	2.209(3)	176.6(11)	177.4(15)	107.8(12)	[30]
[{Ru(PPh ₃) ₂ Cp] ₂ (μ-NCC ₆ H ₄ CN)]PF ₆ 7	2.018(2)	1.146(3)	1.442(4)	2.348(1)	2.344(1)	166.9(2)	176.6(3)	102.89(2)	This work
[{Ru(PPh ₃) ₂ Cp] ₂ (μ-CCC ₆ H ₄ CN)]PF ₆ 9	1.994(5) ^a / 2.020(5) ^b	1.201(7) ^a / 1.146(6) ^b	1.419(7) ^a / 1.415(7) ^b	2.2903(14) ^a / 2.3104(14) ^b	2.3046(13) ^a / 2.3218(14) ^b	172.7(4) ^a / 172.0(4) ^b	175.1(5) ^a / 177.2(5) ^b	99.59(5) ^a / 97.25(5) ^b	This work
10	2.035(2)	1.142(4)	1.442(4)	2.3499(9)	2.3444(8)	176.7(2)	170.5(3)	102.62(3)	This work

^a Data from acetylide coordinated metal centre.

^b Data from nitrile coordinated metal centre.

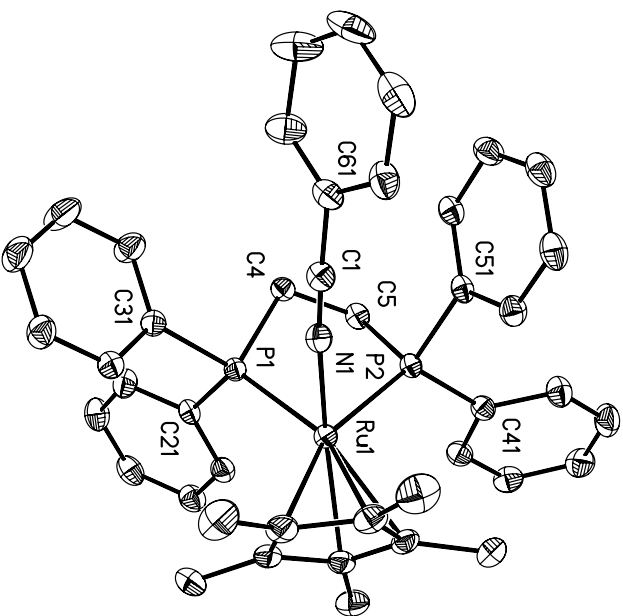


Fig. 1. The cation from **2** illustrating the atom labelling scheme. In this and all subsequent figures, hydrogen atoms and the PF₆ counter ion(s) has been omitted for clarity.

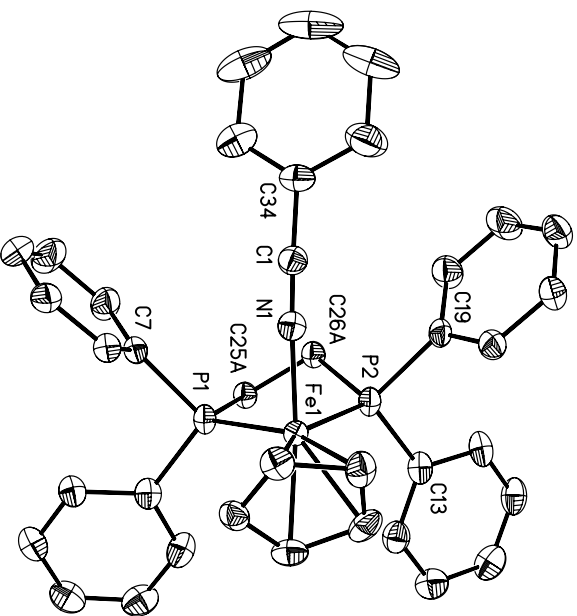


Fig. 2. The complex cation in **3**.

in **5** [1.362(2) Å] is unperturbed from the value found for dimethylaminobenzonitrile [1.365(3) Å] [33,34], and suggests limited contributions from cumulated resonance forms to the overall structure (Fig. 4). The only significant variation in C(1)–C(ipso) bond lengths in the series is observed in the case of **5**, which at 1.424(2) Å is somewhat shorter than the other examples in this series, but essentially identical to that found in the free ligand (1.427(5) Å) [33].

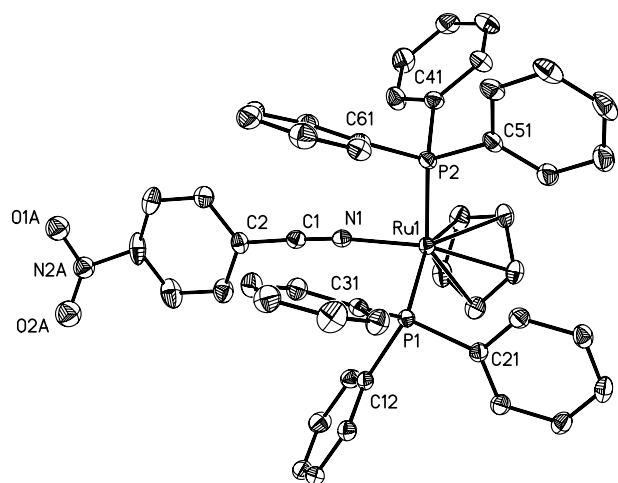


Fig. 3. The cation from **4**. For clarity only one of the disordered positions of the NO_2 is shown.

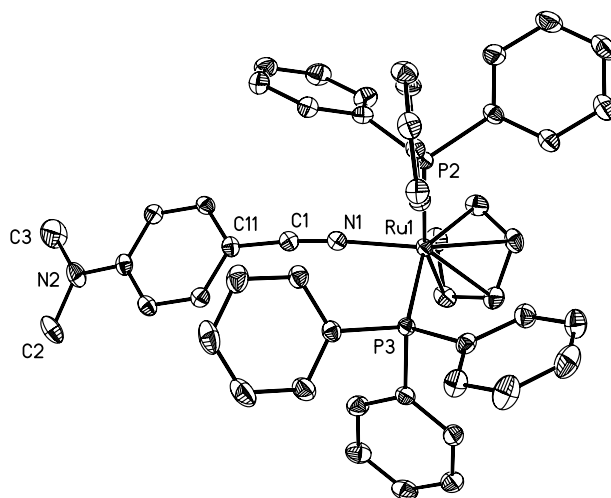


Fig. 4. The cation from the complex salt **5**.

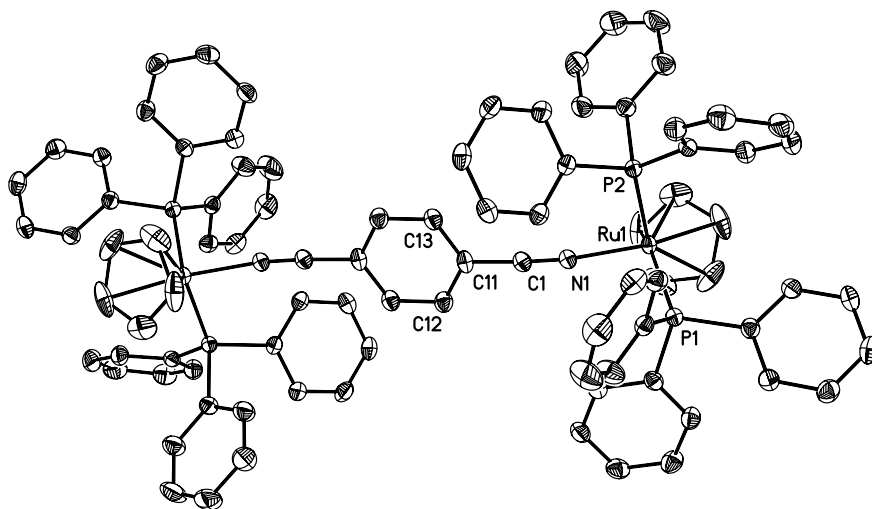


Fig. 5. The bimetallic dication from **7** showing the atom labelling scheme.

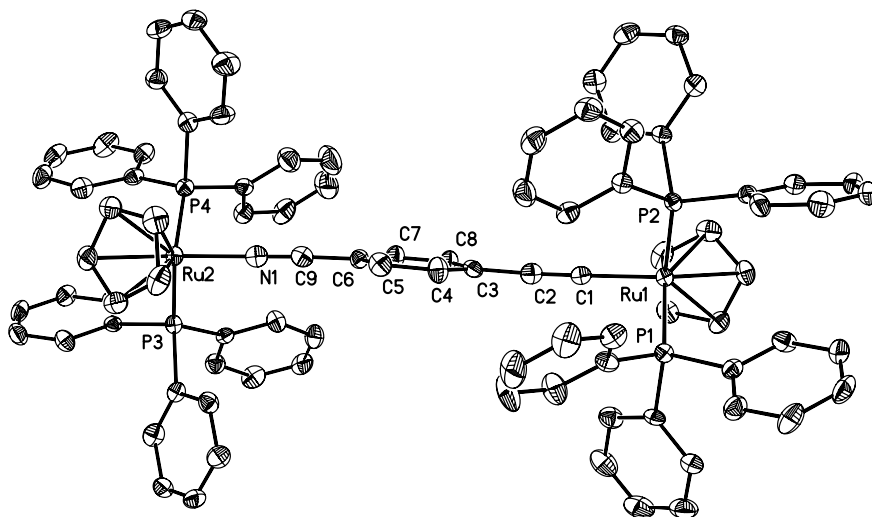


Fig. 6. A plot of the bimetallic cation **9** showing the atom labelling scheme.

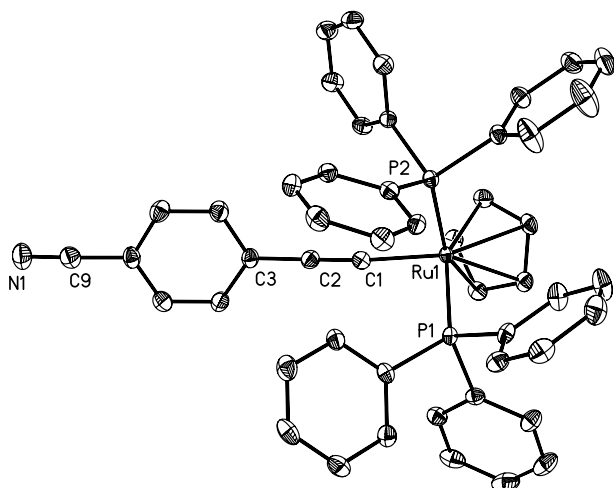


Fig. 7. A plot of a molecule of **6b** showing the atom labelling scheme.

The C–N bond lengths across the series are independent of both the nature of the *para* substituent on the nitrile ligand and the metal fragment and fall in the experimentally indistinguishable range 1.141(3)–1.149(2) Å. The M–N bond distances within the ruthenium based complexes varies between 2.023(2) and 2.041(5) Å. While the shorter Ru–N bond in **4** (which carries an electron accepting NO₂ group) and **2** (which features a more electron donating metal fragment) than in **1**, together with the relative Fe–N bond lengths in **3** and [Fe(NCC₆H₄NO₂)(dppe)Cp]PF₆, is consistent with a back-bonding model, the bond length alone cannot distinguish π -effects from the electrostatic effects highlighted by calculations on Re and Pt based systems [9–11].

The π -accepting properties of phosphines are well established, and consequently within a set of structurally similar complexes the M–P bond length is a modestly sensitive probe of relative electron density at the metal

centres. For example, substitution of the benzonitrile ligand in **1** with a stronger σ -donating ligand such as phenylacetylide [as in Ru(C \equiv CPh)(PPh₃)₂Cp] results in a contraction in the Ru–P bond lengths of approximately 0.1 Å, or about 4%. Similarly, the metal–phosphorus bond lengths display some dependency on the degree of electron density at the metal centre, with the more electron-rich species **2** giving rise to significantly shorter M–P bonds than found in **1** (see above). The trends in Table 4 indicate that the electron-withdrawing NO₂ group has little effect on the M–P bond lengths in either metal acetylide or nitrile complexes. The small contraction of the Ru–P bond lengths in **5** relative to **1** and **4** likely reflects the greater-donating properties of the NMe₂ substituted benzonitrile ligand.

In an effort to more clearly demarcate the electronic properties of the nitrile ligand substituent, we chose to make an altogether less subtle change to the molecular structure and introduced a second metal centre, which would serve as a good σ - and π -donor substituent with little π -acceptor character. In the bimetallic complex **7** (Fig. 5) the metal fragments are related by an inversion centre at the mid-point of the central aromatic ring, and display shorter Ru–N bond lengths and longer Ru–P bond lengths than found in the related monometallic compound **1** (Table 4). The dication **7** also exhibits the greatest deviation from linearity in the M–N–C chain within this series, with the Ru–N(1)–C(1) bond angle being distinctly non-linear (166.9(2)°), although it is most likely that this distortion is due to packing effects rather than any significant anomaly in the electronic structure.

There appears to be little interaction between the metal centres in **7** through the π -system with the N(1)–C(1) and C(1)–C(11) bond lengths being identical with those of **1**. There is no obvious quinoidal character associated with the aromatic portion of the dinitrile ligand. However,

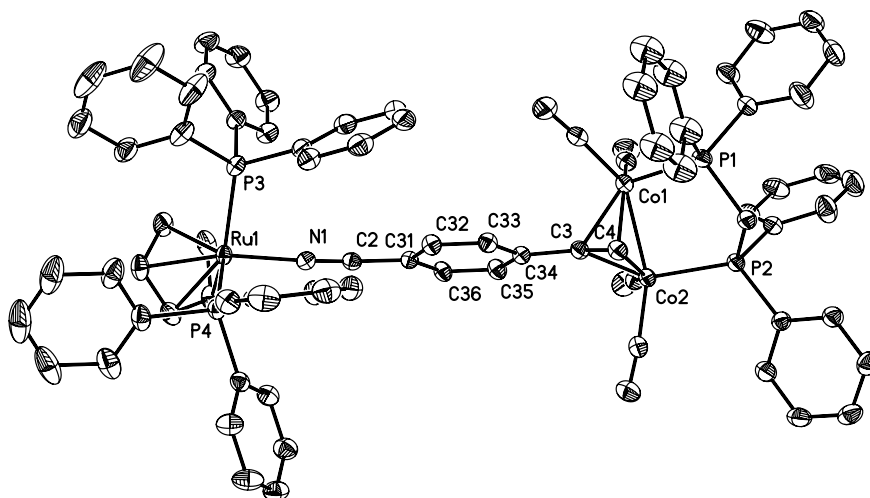


Fig. 8. A plot of the heterometallic cation in **10** showing the atom labelling scheme.

the Ru–N(1) bond lengths are rather short and the Ru–P bond lengths significantly elongated when compared with the monometallic examples. Calculations on Re and Pt systems in which π -back bonding is thought to be negligible suggest that the M–N bond is rather polarised, with a considerable portion of the electronic charge residing on the nitrogen atom. If one takes the elongated Ru–P bond lengths in **7** relative to **1** to be indicative of less electron-rich metal centres, the contraction in the Ru–N bonds can be attributed to the better electrostatic attraction between these centres.

More interesting are the changes that result from dimetallation of 4-ethynylbenzonitrile, and the mixed acetylide/nitrile ligand present in **9** (Fig. 6), together with the structural data from **1**, Ru(C \equiv CPh)(PPh₃)₂Cp and **6b** (Fig. 7), provides the basis for an informative comparison of the metrical parameters associated with the M–C \equiv CR and M–N \equiv CR motifs. Each metal centre in **9** adopts the expected arrangement of Cp and PPh₃ ligands, which together with the acetylide or nitrile fragment give rise to pseudo-octahedral geometry. The aromatic portion of the bridging 4-ethynylbenzonitrile ligand lies in a plane which almost bisects the P–Ru–P angle at each metal centre, and therefore provides a conjugation pathway between d_{π} orbitals on each metal centre. Whilst the C(9) \equiv N(1) and C(1) \equiv C(2) bond lengths in **9** are essentially unchanged relative to the respective model mononuclear complexes, within the C(3)–C(8) ring system there is some evidence for a degree of quinoidal character, which is supported by the short C(2)–C(3) [1.419(7) Å] and C(6)–C(9) [1.415(7) Å] bond lengths.

A comparison of the Ru(1)–P(1,2) bond lengths [2.290(1), 2.305(1) Å] with the Ru–P bond lengths of Ru(C \equiv CPh)(PPh₃)₂Cp [2.229(3), 2.228(3) Å], and of Ru(2)–P(3, 4) [2.310(1), 2.322(1) Å] with those of **1** [2.334(1), 2.335(1) Å] reveals Ru(1)–P(1,2) to be rather elongated in **9**, and the corresponding bonds on the nitrile coordinated metal centre being amongst the shortest reported for this class of complex. When taken as a whole, these structural parameters provide clear evidence for the donation of electron density from Ru(1) to Ru(2) via the polarised σ -bond framework of the ethynylbenzonitrile bridge.

The cluster pendant group in **10** has little influence on the geometry of the ruthenium fragment (Fig. 8). The structure of the Ru(NCR)(PPh₃)₂Cp portion of **10** is essentially identical to that of **1**, save for a small elongation of the Ru–P bond lengths and expansion of the P–Ru–P angle in the case of the cluster complex. The small differences in the structural parameters in related acetylide complexes have been commented upon previously [35].

3. Conclusion

Structural data from a series of half-sandwich metal complexes featuring substituted benzonitrile ligands are inconsistent with a significant contribution from metal to

nitrile π -back bonding effects to the M–N coordinate bond. The variations in structure are more sensitive to σ -donating substituents, in agreement with recent computational work on rhenium and platinum complexes.

4. Experimental

All reactions were carried out in dry solvents, purified using an Innovative Technology solvent purification system, in oven dried glassware under an atmosphere of nitrogen as a routine precaution. The complexes RuCl(PPh₃)₂Cp [39], RuCl(dppe)Cp* [40], FeCl(dppe)Cp [41], and Co₂(μ, η^2 -HC₂C₆H₄CN-4)(CO)₄(dppm) [35] were prepared as described previously. Commercial benzonitrile was distilled prior to use, other reagents were used as received. IR spectra were recorded from nujol mulls on NaCl plates using a Nicolet Avatar spectrometer fitted with an MCT detector (2 cm⁻¹ resolution). NMR spectra were recorded on Varian Unity – 300 (¹H, 299.91 MHz; ³¹P, 121.40 MHz) or INOVA 500 (¹³C, 125.69 MHz) spectrometers from solutions in CDCl₃ unless indicated otherwise, and referenced against residual solvent resonances or an external H₃PO₄ reference. Electrochemical measurements were made from solutions in CH₂Cl₂ containing 0.1 M NBu₄BF₄ supporting electrolyte, using a conventional three electrode cell and recorded on an AutoLab PGSTAT-30 potentiostat. A platinum dot working electrode was employed together with Pt wire counter and pseudo reference electrodes. All potentials are reported against SCE, being referenced against an internal ferrocene/ferrrocenium couple (0.46 V).

4.1. Preparation of [Ru(NCC₆H₅)(PPh₃)₂Cp][PF₆] (**1**)

A flask was charged with RuCl(PPh₃)₂Cp (250 mg, 0.345 mmol), benzonitrile (0.1 ml, 0.97 mmol), and NH₄PF₆ (200 mg, 1.22 mmol). The solids were suspended in MeOH (20 ml) and the mixture heated to reflux under a nitrogen atmosphere. After 30 min the yellow solution that had formed was allowed to cool to room temperature and was then further cooled using an ice/water bath. The resulting yellow precipitate was collected by filtration and washed with cold methanol to give **1** as a yellow solid (146 mg, 0.156 mmol, 45%). Crystals suitable for X-ray diffraction studies were obtained by slow diffusion of MeOH into a CH₂Cl₂ solution of **1**. Found: C, 61.29; H, 4.30; N, 1.52. RuC₄₈H₄₀P₃F₆N requires: C, 61.41; H, 4.29; N, 1.49. ¹H NMR: δ 4.55 (s, 5H, Cp); 7.09–7.57 (m, 35H, Ph). ¹³C {¹H} NMR: δ 135.9 (m, J_{CP} = 23 Hz, C_{ipso} PPh₃); 133.8 (s, C4); 133.5 (t, J_{CP} = 5 Hz, C_{ortho} PPh₃); 132.7 (s, C2); 130.4 (s, C_{para} PPh₃); 129.5 (s, C3); 128.7 (t, J_{CP} = 5 Hz, C_{meta} PPh₃); 111.5 (s, C1); 84.4 (s, Cp). ³¹P {¹H} NMR: δ 42.9 (s, PPh₃); –143 (ht, J_{PF} = 713 Hz PF₆). ES(+)-MS (m/z): 794 [Ru(NCC₆H₅)(PPh₃)₂Cp]⁺; 691 [Ru(PPh₃)₂Cp]⁺. IR: ν (C \equiv N) 2233 cm⁻¹.

4.2. Preparation of $[Ru(NCC_6H_5)(dppe)Cp^*][PF_6]$ (**2**)

In a manner similar to that described for the preparation of **1**, a suspension of $RuCl(dppe)Cp^*$ (200 mg, 0.299 mmol), benzonitrile (0.1 ml, 0.97 mmol), and NH_4PF_6 (195 mg, 1.20 mmol) in refluxing MeOH (10 ml) was allowed to react for 1 h. The resulting yellow solution was cooled to room temperature and solvent removed. The yellow residue was dissolved in the minimum quantity of CH_2Cl_2 , filtered and the product crystallised by slow diffusion of hexane into a CH_2Cl_2 solution, affording yellow crystals of **2** (207 mg, 0.235 mmol, 78%). This compound repeatedly analysed low in carbon. 1H NMR (CD_2Cl_2): δ 1.51 (s, 15H, Cp^*); 2.46, 2.50 (2 \times br, 4H, dppe); 6.54, 6.57 (pseudo-d, 2H_{ortho}, PhCN); 7.26–7.62 (m, 23H, Ph). ^{13}C { 1H } NMR (CD_2Cl_2): δ 134.6–126.2 (m, Ph); 111.3 (s, C \equiv N); 93.2 (s, C_5Me_5); 28.8–28.4 (m, dppe); 9.7 (s, C_5Me_5). ^{31}P { 1H } NMR (CD_2Cl_2): δ 76.2 (s, dppe); –143.4 (ht, $J_{PF} = 710$ Hz PF_6). ES(+)-MS (m/z): 794 $[Ru(NCC_6H_5)(dppe)Cp^*]^+$; 635 $[Ru(dppe)Cp^*]^+$. IR: $\nu(C\equiv N)$ 2227 cm^{-1} .

4.3. Preparation of $[Fe(NCC_6H_5)(dppe)(Cp)][PF_6]$ (**3**)

An analogous procedure using $FeCl(dppe)(Cp)$ (200 mg, 0.361 mmol), benzonitrile (0.1 ml, 0.97 mmol) and NH_4PF_6 (235 mg, 1.44 mmol) followed by recrystallisation by diffusion of MeOH into a CH_2Cl_2 solution resulted in the formation of red crystals of **3** (163 mg, 0.213 mmol, 59%). Found: C, 59.87; H, 4.45; N, 1.80. $C_{38}H_{34}P_3NF_6Fe$ requires: C, 59.47; H, 4.47; N, 1.82. 1H NMR: δ 4.45 (s, 5H, Cp); 2.45, 2.63 (2 \times br, 4H, dppe); 6.46 (s, 2H_{ortho}, PhCN); 7.16–7.86 (m, 23H, Ph). ^{13}C { 1H } NMR: δ 136.7 (m, 2 \times C_{ipso}); 134.3 (s, C_4); 133.4 (s, C_2); 133.0 (br, C_{ortho}); 132.0 (s, C_3); 131.5 (br, C_{ortho}); 131.3 (s, C_{para}); 130.9 (s, C_{para}); 129.7 (br, C_{meta}); 129.5 (br, C_{meta}); 129.1 (s, CN); 111.4 (s, C_1); 79.9 (s, Cp); 28.1 (m, dppe). ^{31}P { 1H } NMR: δ 98.3 (s, dppe); –143.1 (ht, $J_{PF} = 713$ Hz PF_6). ES(+)-MS (m/z): 622 $[Fe(NCC_6H_5)(dppe)Cp]^+$; 519 $[Fe(dppe)Cp]^+$. IR: $\nu(C\equiv N)$ 2217 cm^{-1} .

4.4. Preparation of $[Ru(NCC_6H_4NO_2)(PPh_3)_2Cp][PF_6]$ (**4**)

The reaction between $RuCl(PPh_3)_2Cp$ (100 mg, 0.138 mmol), 4-nitrobenzonitrile (20.4 mg, 0.138 mmol), and NH_4PF_6 (80 mg, 0.49 mmol) in refluxing MeOH (20 ml) afforded an orange solution after 30 min which was cooled (ice/water) to afford **4** as an orange precipitate (90 mg, 0.092 mmol, 66%). Crystals suitable for X-ray diffraction studies were obtained from slow diffusion of MeOH into a solution of **4** in CH_2Cl_2 . Found: C, 54.57; H, 3.84; N, 2.66. $RuC_{49}H_{41}N_2P_3F_6Cl_2O_2$ requires: C, 55.07; H, 3.87; N, 2.62. 1H NMR: δ 4.64 (s, 5H, Cp); 7.11–7.39 (m, 40H, Ph). ^{13}C { 1H } NMR: δ 150.0 (s, C_4) 135.6 (m, $J_{CP} = 22$ Hz, C_{ipso} PPh₃); 134.21 (s, C_2) 133.5 (t, $J_{CP} = 5$ Hz, C_{ortho} PPh₃); 130.5 (s, C_{para}); 128.8 (t, $J_{CP} = 5$ Hz, C_{meta} PPh₃); 127.9 (s, CN); 124.3 (s, C_3);

117.5 (s, C_1); 85.0 (s, Cp). ^{31}P { 1H } NMR: δ 43.0 (s, PPh₃); –142.9 (ht, $J_{PF} = 713$ Hz PF_6). ES(+)-MS (m/z): 839 $[Ru(NCC_6H_4NO_2)(PPh_3)_2Cp]^+$; 691 $[Ru(PPh_3)_2Cp]^+$. IR: $\nu(C\equiv N)$ 2228 cm^{-1} .

4.5. Preparation of $[Ru(NCC_6H_4NMe_2)(PPh_3)_2Cp][PF_6]$ (**5**)

Reaction of $RuCl(PPh_3)_2Cp$ (100 mg, 0.138 mmol), 4-*N,N*-dimethylaminobenzonitrile (20 mg, 0.138 mmol), and NH_4PF_6 (80 mg, 0.49 mmol) yielded **5** as a yellow solid (65 mg, 0.066 mmol, 48%). Crystals suitable for X-ray diffraction were obtained from slow diffusion of hexane into a solution of **5** in $CHCl_3$. Found: C, 60.69; H, 4.61; N, 2.84. $RuC_{50}H_{45}N_2P_3F_6$ requires: C, 61.16; H, 4.62; N, 2.85. 1H NMR: δ 4.42 (s, 5H, Cp); 7.00–7.30 (m, 37H, Ph); 2.97 (s, 6H, N(CH₃)₂). ^{13}C { 1H } NMR: δ 153.2 (s, C_4) 136.1 (t, $J_{CP} = 23$ Hz, C_{ipso} PPh₃); 133.8 (s, C_2) 133.48 (t, $J_{CP} = 5$ Hz, C_{ortho} PPh₃); 130.3 (s, C_{para}); 128.6 (t, $J_{CP} = 5$ Hz, C_{meta} PPh₃); 111.8 (s, C_3); 95.6 (s, C_1); 83.8 (s, Cp); 40.2 (s, Me). ^{31}P { 1H } NMR: δ 42.8 (s, PPh₃); –143.0 (ht, $J_{PF} = 713$ Hz PF_6). ES(+)-MS (m/z): 837 $[Ru(NCC_6H_4NMe_2)(PPh_3)_2Cp]^+$; 691 $[Ru(PPh_3)_2Cp]^+$. IR: $\nu(C\equiv N)$ 2221 cm^{-1} .

4.6. Preparation of $[Ru(NCC_6H_4CN-4)(PPh_3)_2Cp][PF_6]$ (**6a**)

A flask was charged with $RuCl(PPh_3)_2Cp$ (100 mg, 0.138 mmol), 1,4-dicyanobenzene (173 mg, 1.38 mmol), and NH_4PF_6 (80 mg, 0.49 mmol). Methanol (20 ml) was added and the suspension was heated to reflux under a nitrogen atmosphere. After 30 min the yellow solution was cooled and the solvent removed on a rotary evaporator. The yellow residue was dissolved in the minimum quantity of CH_2Cl_2 , filtered and precipitated into Et₂O. The precipitate formed was collected and dried to obtain **6a** as a pale yellow powder (100 mg, 0.104 mmol, 75%), but could not be obtained in an analytically pure form, presumably due to the complications of disproportionation described in the text. 1H NMR: δ 4.62 (s, 5H, Cp); 6.98–7.37 (m, 74H, Ph). ^{31}P { 1H } NMR: δ 42.6 (s, PPh₃); –142.9 (ht, $J_{PF} = 713$ Hz, PF_6). ES(+)-MS (m/z): 819 $[Ru(NCC_6H_4CN)(PPh_3)_2Cp]^+$; 691 $[Ru(PPh_3)_2Cp]^+$. IR: $\nu(C\equiv N)$ 2221 cm^{-1} .

4.7. Preparation of $Ru(CCC_6H_4CN)(PPh_3)_2Cp$ (**6b**)

A suspension of $RuCl(PPh_3)_2Cp$ (200 mg, 0.275 mmol), $HC\equiv CC_6H_4CN$ (150 mg, 1.18 mmol), and NH_4PF_6 (100 mg, 0.61 mmol) in methanol (20 ml) was heated to reflux under a nitrogen atmosphere. After 1 h the red solution formed was treated with DBU and the yellow precipitate formed was collected and washed (MeOH) and dried to give **6b** as a bright yellow powder (202 mg, 0.247 mmol, 90%). Despite repeated efforts, the compound analysed consistently low in carbon (ca. 0.8%). 1H NMR: δ

4.31 (s, 5H, Cp); 7.43–6.99 (m, 34H, Ph). ^{31}P { ^1H } NMR: δ 51.3 (s, PPh₃). ES(+)-MS (m/z): 818 [M + H]⁺; 691 [Ru(PPh₃)₂Cp]⁺. IR: $\nu(\text{C}\equiv\text{N})$ 2220 cm⁻¹, $\nu(\text{C}\equiv\text{C})$ 2063, 2037(sh) cm⁻¹.

4.8. Preparation of [$\{\text{Ru}(\text{PPh}_3)_2\text{Cp}\}_2(\mu\text{-}1,4\text{-NCC}_6\text{H}_4\text{-CN})$][PF₆]₂ (**7**)

The reaction of RuCl(PPh₃)₂Cp (200 mg, 0.276 mmol), 1,4-dicyanobenzene (18 mg, 0.136 mmol), and NH₄PF₆ (160 mg, 0.98 mmol) in the usual manner yielded **7** as a yellow solid (140 mg, 0.078 mmol, 57%) which was recrystallised from CH₂Cl₂/MeOH. Found: C, 56.03; H, 3.79; N, 1.40. Ru₂C₉₂H₇₈N₂P₆F₁₂Cl₄ requires: C, 56.11; H, 3.99; N, 1.42. ^1H NMR: δ 4.57 (s, 10H, Cp); 6.98–7.37 (m, 74H, Ph). ^{31}P { ^1H } NMR: δ 42.6 (s, PPh₃); -142.8 (ht, $J_{\text{PF}_6} = 713$ Hz, PF₆). ES(+)-MS (m/z): 1655 [M - PF₆]⁺; 819 [Ru(NCC₆H₄CN)(PPh₃)₂Cp]⁺; 691 [Ru(PPh₃)₂Cp]⁺. IR: $\nu(\text{C}\equiv\text{N})$ 2226 cm⁻¹.

4.9. Preparation of [$\{\text{Fe}(\text{dppe})\text{Cp}\}_2(\mu\text{-NCC}_6\text{H}_4\text{CN-}4)$][PF₆]₂ (**8**)

A solution of FeCl(dppe)Cp (150 mg, 0.27 mmol) and 1,4-dicyanobenzene (17.3 mg, 0.13 mmol) in THF (15 ml) was treated with NH₄PF₆ (90 mg, 0.55 mmol) and the dark blue-black solution heated at reflux point for 2 h, during which time a red precipitate gradually formed. The solid was collected by filtration, and washed with hexane before being recrystallised from CH₂Cl₂ and diethyl ether, affording the title material (63 mg, 0.043 mmol, 32%). Found: C, 55.31; H, 4.20; N, 1.87. Fe₂C₇₁H₆₄N₂P₆F₁₂Cl₂ requires: C, 55.31; H, 4.18; N, 1.82. ^1H NMR: δ 2.42, 2.60 (2 × m, 2 × 2H, dppe); 4.47 (s, 5H, Cp); 5.32 (CH₂Cl₂ of recrystallisation, 1H); 6.24 (s, 2H, NCC₆H₄CN); 7.32–7.78 (m, 20H, Ph). ^{13}C NMR: δ 136.5 (t, $J_{\text{CP}} = 19$ Hz, C_{ipso} dppe); 136.2 (t, $J_{\text{CP}} = 19$ Hz, C_{ipso} dppe); 132.9 (t, $J_{\text{CP}} = 5$ Hz, C_{ortho} dppe); 132.0 (s, C_{para} dppe); 131.4 (t, $J_{\text{CP}} = 5$ Hz, C_{ortho} dppe); 131.3 (s, C2/C3); 131.0 (s, C2/C3); 129.6 (t, $J_{\text{CP}} = 5$ Hz, C_{meta} dppe); 129.5 (t, $J_{\text{CP}} = 5$ Hz, C_{meta} dppe); 114.7 (s, C1); 80.5 (s, Cp), 28.0 (m, dppe). ^{31}P { ^1H } NMR: δ 97.9 (s, dppe). ES(+)-MS (m/z): 1311, [M - PF₆]⁺; 519, [Fe(dppe)Cp]⁺. IR: $\nu(\text{C}\equiv\text{N})$ 2223 cm⁻¹.

4.10. Preparation of [$\{\text{Ru}(\text{PPh}_3)_2\text{Cp}\}_2(\mu\text{-CCC}_6\text{H}_4\text{CN-}4)$](PF₆) (**9**)

A suspension of RuCl(PPh₃)₂Cp (200 mg, 0.275 mmol), HC≡CC₆H₄CN (18 mg, 0.142 mmol), and NH₄PF₆ (70 mg, 0.43 mmol) in methanol (20 ml) was heated at reflux point under a nitrogen atmosphere. After 30 min the orange solution formed was treated with a methanolic solution of NaOMe and refluxed for a further 30 min. The yellow precipitate formed was collected and washed with MeOH and hexane and dried to give **9** as a yellow powder (180 mg, 0.11 mmol, 80%). Found: C, 65.48; H, 4.48; N, 1.03. Ru₂C₉₁H₇₄NP₅F₆.2C₃H₆O requires: C, 65.87; H,

4.90; N, 0.79. ^1H NMR: δ 4.52 (s, 5H, Cp); 4.35 (s, 5H, Cp); 7.41–6.96 (m, 64H, Ph). ^{31}P { ^1H } NMR: δ 51.3 (s, PPh₃); 42.8 (s, PPh₃); -143.0 (ht, $J_{\text{PF}_6} = 713$ Hz, PF₆). ES(+)-MS (m/z): 1508 [Ru(PPh₃)₂Cp]₂(μ-C≡CC₆H₄CN-4)]⁺, 818 [Ru(C≡CC₆H₄CN)(PPh₃)₂Cp + H]⁺; 691 [Ru(PPh₃)₂Cp]⁺. IR: $\nu(\text{C}\equiv\text{N})$ 2218 cm⁻¹, $\nu(\text{C}\equiv\text{C})$ 2059, 2040(sh) cm⁻¹.

4.11. Preparation of [$\text{Co}_2(\mu,\eta^2\text{-HC}_2\text{C}_6\text{H}_4\text{CN-}4)\text{-}\{\text{Ru}(\text{PPh}_3)_2\text{Cp}\}(\text{CO})_4(\text{dpmm})$](PF₆) (**10**)

A solution of RuCl(PPh₃)₂Cp (97.9 mg, 0.135 mmol), Co₂(μ,η²-HC₂C₆H₄CN-4)(CO)₄(dpmm) (100 mg, 0.135 mmol), and NH₄PF₆ (80 mg, 0.49 mmol), were allowed to react in refluxing MeOH (15 ml) and THF (5 ml) for 2.5 h after which time the solvent was removed and the residue recrystallised from CH₂Cl₂/MeOH affording **10** as dark red crystals (141 mg, 0.089 mmol, 66C₈₀H₆₄Co₂RuO₄P₅NF₆Cl₂ requires: C, 57.81; H, 3.88; N, 0.84. ^1H NMR: δ 3.06 (dt, 1H, $J_{\text{HP}} = 13$ Hz, $J_{\text{HH}} = 9$ Hz, CHP_2); 3.60 (dt, 1H, $J_{\text{HP}} = 13$ Hz, $J_{\text{HH}} = 10$ Hz, CHP_2); 4.47 (s, 5H, Cp); 5.80 (s, 1H, $J_{\text{HP}} = 7$ Hz, Co₂C₂H); 7.05–7.50 (m, 54H, Ph). ^{13}C { ^1H } NMR: δ 84.0 (s, Cp); 128.5–133.2 (m, Ph). ^{31}P { ^1H } NMR: δ 42.8 (s, dpmm); 43.8 (br, PPh₃). ES(+)-MS (m/z): 1432 [Co₂(μ,η²-HC₂C₆H₄CN-4){Ru(PPh₃)₂Cp}(CO)₄(dpmm)]⁺; 691 [Ru(PPh₃)₂Cp]⁺. IR: $\nu(\text{CO})$ 2021, 1993, 1973 1955 cm⁻¹. The $\nu(\text{CN})$ band could not be detected.

4.12. Crystallographic studies

Diffraction data were collected on Bruker 3-circle diffractometers with SMART 6K (for **2**, **3**, **5** and **7**) or SMART 1K (for **4**, **6b**, **9** and **10**) CCD area detectors, using graphite-monochromated sealed-tube Mo K α radiation. The data collection was carried out at 120 K (for **2**, **3**, **4**, **5**, **6b**, **7** and **9**) and 100 K (for **10**) using cryostream (Oxford cryosystem) open flow N₂ cryostats. Reflection intensities were integrated using the SAINT V6.45 program [42] (for **2**, **3**, **5** and **9**) and SAINT V6.02a [43] (for **4**, **6b**, **7** and **10**).

The crystal structures were solved using direct-methods and refined by full matrix least-squares against F^2 of all data using SHELXTL [44] software. All non-hydrogen atoms were refined in anisotropic approximation, except the disordered nitro group in **4** and the carbon atom of a dichloromethane molecule in **10**, which were isotropically refined. Hydrogen atoms were either located by a difference map (for **2**, **3**, **5** and **7**) or placed in calculated positions (**4**, **6b**, **9** and **10**) and refined isotropically using a riding model. For compound **10** the position of the hydrogen atom (H4) in the dicobalt moiety was freely refined.

Disorder is present in all the structures except **6b** and **7**. The PF₆ anion is disordered in compounds **2**, **5**, and **9**. In the crystal structure of **3**, the alkane chain of the dppe moiety is disordered between two positions, partially populated with occupancies of ca. 0.8 and 0.2. The nitro group in compound **4** is highly disordered, and the electron density

distribution was modeled by locating this group at three different positions. In compound **10**, a phenyl ring of the dppm moiety presents rotational disorder. In the crystal structure of **2**, disordered solvent molecules are present, and Platon's Squeeze tool was applied [45]. Crystal data and experimental details are listed in Table 3.

5. Supplementary information

Crystallographic data for the structural analysis has been deposited with the Cambridge Crystallographic Data Centre, CCDC Nos. 259771–259778 for compounds **2**, **3**, **5**, **4**, **6b**, **10**, **7**, and **9** respectively.

Acknowledgements

We are grateful to the EPSRC, ONE-North East and the University of Durham for financial support of this work and to Johnson Matthey Plc for a generous loan of $\text{RuCl}_3 \cdot n\text{H}_2\text{O}$. RLC and RLR hold studentships from the Department of Chemistry's EPSRC Doctoral Training Account.

References

- [1] J.A. Mata, E. Peris, S. Uriel, R. Llusar, I. Asselberghs, A. Persoons, *Polyhedron* 20 (2001) 2083.
- [2] A.R. Dias, M.-H. Garcia, J.C. Rodrigues, J.C. Petersen, T. Bjornholm, T. Geisler, *J. Mater. Chem.* 5 (1995) 1861.
- [3] J.F. Costello, S.G. Davies, R.M. Highcock, M.E.C. Polywka, M.W. Poulter, T. Richardson, G.G. Roberts, *J. Chem. Soc., Dalton Trans.* (1997) 105.
- [4] A.R. Dias, M.H. Garcia, J.C. Rodrigues, M.L.H. Green, S.M. Kuebler, *J. Organomet. Chem.* 475 (1994) 241.
- [5] M.H. Garcia, M.P. Robalo, A.R. Dias, M.T. Duarte, W. Wenseleers, G. Aerts, E. Goovaerts, M.P. Cifuentes, S. Hurst, M.G. Humphrey, M. Samoc, B. Luther-Davies, *Organometallics* 21 (2001) 2107.
- [6] A.R. Dias, M.H. Garcia, M.P. Robalo, M.L.H. Green, K.K. Lai, A.J. Pulham, S.M. Kuebler, G. Balavoine, *J. Organomet. Chem.* 453 (1993) 241.
- [7] W. Wenseleers, A.W. Gerbrandij, E. Goovaerts, M.H. Garcia, M.P. Robalo, P.J. Mendes, J.C. Rodrigues, A.R. Dias, *J. Mater. Chem.* 8 (1998) 925.
- [8] M.H. Garcia, J.C. Rodrigues, A.R. Dias, M.F.M. Piedade, M.T. Duarte, M.P. Robalo, N. Lopes, *J. Organomet. Chem.* 632 (2001) 133.
- [9] M.L. Kuznetsov, A.J.L. Pombeiro, *Dalton Trans.* (2003) 738.
- [10] M.L. Kuznetsov, E.A. Klestova-Nadeeva, A.I. Dement'ev, *J. Mol. Struct. – Theochem.* 671 (2004) 229.
- [11] M.L. Kuznetsov, *J. Mol. Struct. – Theochem.* 674 (2004) 33.
- [12] A.V. George, L.D. Field, E.Y. Malouf, A.E.D. McQueen, S.R. Pike, G.R. Purches, T.W. Hambley, I.E. Buys, A.H. White, D.C.R. Hockless, B.W. Skelton, *J. Organomet. Chem.* 538 (1997) 101.
- [13] N.J. Long, C.K. Williams, *Angew. Chem., Int. Ed.* 42 (2003) 2586.
- [14] F. Paul, C. Lapinte, *Coord. Chem. Rev.* 178–180 (1998) 431.
- [15] I.R. Whittall, A.M. McDonagh, M.G. Humphrey, *Adv. Organomet. Chem.* 43 (1999) 349.
- [16] I.R. Whittall, A.M. McDonagh, M.G. Humphrey, *Adv. Organomet. Chem.* 42 (1998) 291.
- [17] G.S. Ashby, M.I. Bruce, B.I. Tomkins, R.C. Wallis, *Aust. J. Chem.* 32 (1979) 1003.
- [18] M.I. Bruce, M.A. Buntine, K. Costuas, B.G. Ellis, J.F. Halet, P.J. Low, B.W. Skelton, A.H. White, *J. Organomet. Chem.* 689 (2004) 3308.
- [19] R.L. Cordiner, D. Corcoran, D.S. Yufit, A.E. Goeta, J.A.K. Howard, P.J. Low, *Dalton Trans.* (2003) 3541.
- [20] T. Richardson, G.G. Roberts, M.E.C. Polywka, S.G. Davies, *Thin Solid Films* 160 (1998) 231.
- [21] J.F. Costello, S.G. Davies, R.M. Highcock, M.E.C. Polywka, M.W. Poulter, T. Richardson, G.G. Roberts, *J. Chem. Soc., Dalton Trans.* (1997) 105.
- [22] D.S. Pandey, R.L. Mishra, A. Mishra, U.C. Agarwala, *Polyhedron* 9 (1990) 2153.
- [23] R. Denis, L. Toupet, F. Paul, C. Lapinte, *Organometallics* 19 (2000) 4240.
- [24] I.R. Whittall, M.G. Humphrey, D.C.R. Hockless, B.W. Skelton, A.H. White, *Organometallics* 14 (1995) 3970.
- [25] N.G. Connelly, W.E. Geiger, *Chem. Rev.* 96 (1996) 877.
- [26] D.E. Richardson, H. Taube, *Inorg. Chem.* 20 (1981) 1278.
- [27] N. Le Narvor, C. Lapinte, *Organometallics* 14 (1995) 634.
- [28] H.C. Aspinall, A.J. Deeming, S. Donovan-Mtzuni, *J. Chem. Soc. Dalton Trans.* (1983) 2669.
- [29] C. Díaz, I. Izquierdo, F. Mendizábal, N. Yutronic, *Inorg. Chim. Acta* 284 (1999) 20.
- [30] M.H. Garcia, M.P. Robalo, A.R. Dias, M.F.M. Piedade, A. Galvão, W. Wenseleers, E. Goovaerts, *J. Organomet. Chem.* 619 (2001) 252.
- [31] T. Higashi, K. Osaki, *Acta Crystallogr., Sect. B Struct. Crystallogr. Cryst. Chem.* 33 (1977) 2337.
- [32] M.A.A.F. de C.T. Carrondo, A.R. Dias, M.H. Garcia, P.M. Maitlis, M.P. Robalo, M.L.H. Green, J. Higgins, Y.Y. Yang, *J. Organomet. Chem.* 395 (1990) 279.
- [33] A. Heine, R. Herbst-Irmer, D. Stalke, W. Kühnle, K.A. Zachariasse, *Acta Crystallogr. B* 50 (1994) 363.
- [34] A. Gourdon, J.-P. Launay, M. Bujoli-Doeuff, F. Heisel, J.A. Miehe, E. Amouyal, M.-L. Boillot, *J. Photochem. Photobiol. A Chem.* 71 (1993) 13.
- [35] T.J. Snaith, P.J. Low, R. Rousseau, H. Puschmann, J.A.K. Howard, *J. Chem. Soc., Dalton Trans.* (2001) 292.
- [36] G. Fauvet, M. Massauz, R. Chevalier, *Acta Crystallogr. B* 34 (1978) 1376.
- [37] J.M. Wisner, T.J. Bartczak, J.A. Albers, *Inorg. Chim. Acta* 100 (1985) 115.
- [38] M.I. Bruce, M.G. Humphrey, M.R. Snow, E.R.T. Tiekink, *J. Organomet. Chem.* 314 (1986) 213.
- [39] M.I. Bruce, N.J. Windsor, *Aust. J. Chem.* 30 (1977) 1601.
- [40] M.I. Bruce, B.G. Ellis, P.J. Low, B.W. Skelton, A.H. White, *Organometallics* 22 (2003) 3184.
- [41] M.J. Mays, P.L. Sears, *J. Chem. Soc., Dalton Trans.* (1973) 1873.
- [42] SAINT V6.45, Bruker AXS, Madison, WI, USA, 2001.
- [43] SAINT V6.02a, Bruker AXS, Madison, WI, USA, 2000.
- [44] SHELXTL, version 5.10, Bruker AXS, Madison, WI, USA, 1997.
- [45] A.L. Spek, *J. Appl. Crystallogr.* 33 (2003) 7.